



Cite this: DOI: 10.1039/d4cc04623d

Received 9th September 2024,
Accepted 21st October 2024

DOI: 10.1039/d4cc04623d

rsc.li/chemcomm

Solid-state synthesis of ligand-assisted lead halide nanoclusters†

David C. Zeitz, Kai-Chun Chou and Jin Z. Zhang *

A solid-state synthesis of blue-emitting lead halide nanoclusters has been demonstrated for the first time. The solid-state grinding synthesis provides a facile method to produce highly confined lead bromide clusters under ambient conditions. Both $\text{CH}_3\text{NH}_3\text{PbBr}_3$ perovskite magic-sized clusters and lead halide molecular clusters have been produced, as confirmed by comparison to those synthesized using a ligand-assisted reprecipitation method in terms of electronic absorption, photoluminescence, and solid state characterization.

Lead halide perovskites are of an ABX_3 composition where the A component is a monovalent cation like Cs^+ or CH_3NH_3^+ (MA^+), the B component is Pb^{2+} , and the X component is a halide (Cl^- , Br^- , or I^-). Perovskite quantum dots (PQDs) have been subject to deep study over the past several decades due to their attractive properties, such as their size and composition dependent absorption and emission through the visible range.^{1–5} This tunability is governed by the quantum confinement effect (QCE), where, as a decreasing particle size approaches the Bohr radius, it is associated with increasingly blue absorption and emission.^{1,3,6,7} While PQDs with size larger than 4.0 nm have been well studied, much less is known about more highly quantum confined perovskite systems with smaller size.^{7,8}

One such system is the perovskite magic sized cluster (PMSC), also with ABX_3 composition, but with a size approaching 2.0 nm.^{9,10} This much smaller size results in a significant blue shift of the optical absorption and emission bands to about 420 nm compared to PQDs like MAPbBr_3 and CsPbBr_3 which have bands around 500 nm.^{11–13} Similarly, ligand-assisted metal halide molecular clusters (MHMCs) of PbBr_2 , which lack the perovskite A component, show first excitonic absorption around 400 nm and a size around 1.5 nm.^{10,14,15} These clusters exhibit several novel properties compared to

PQDs. For example, MHMCs have recently been studied in terms of their ultrafast excited state dynamics, which indicate a shorter exciton lifetime compared to PQDs.¹⁶ Also, when using achiral passivating ligands, both PMSCs and MHMCs have been demonstrated to display a circular dichroism (CD) signal that PQDs do not, suggesting that these novel clusters have intrinsically chiral properties.^{17,18} These studies indicate that the size of a nanocluster has a fundamental impact on its properties.

To date, PMSCs and MHMCs have only been synthesized using ligand-assisted reprecipitation (LARP), making solid-state characterization difficult, as samples from solution synthesis are challenging to study as solids.^{9,10,15} This difficulty is due to the nanoclusters small size making them difficult to isolate from a colloid, and, if collected, their tendency to aggregate upon drying.¹² Thus, new and simpler synthetic methods are desired.

In this work, a solid-state grinding method was demonstrated to remove the synthetic reliance on solvents and to allow for greater ease of solid-state characterization. Although this work primarily focuses on the synthesis and characterization of MHMCs, the robustness of the proposed method was explored through the synthesis of PMSCs. Successful synthesis of these distinct, highly confined nanostructures in ambient conditions and without solvent-assisted methods indicates that greater methodological diversity is possible than currently represented in the literature.

The MHMC synthesis proceeded by the addition of 0.200 mmol (73.0 mg) of PbBr_2 and 2.00 mmol (183 μL) of butyric acid (BTA) to an agate mortar where they were ground for five minutes. Next, 2.00 mmol (198 μL) of butylamine (BTYA) was added and ground for an additional five minutes, yielding a white product with dark blue luminescence. The prepared product was then suspended in 5.00 mL of toluene followed by further dilution at a rate of 1.00 mL product to 5.00 mL toluene, where the diluted colloid was retained for optical characterization. MHMC purification procedures and PMSC solid state syntheses are available in the ESI,† along with

Department of Chemistry and Biochemistry, University of California, Santa Cruz, California 95064, USA. E-mail: zhang@ucsc.edu

† Electronic supplementary information (ESI) available: Detailed synthetic and experimental procedures and additional spectra. See DOI: <https://doi.org/10.1039/d4cc04623d>

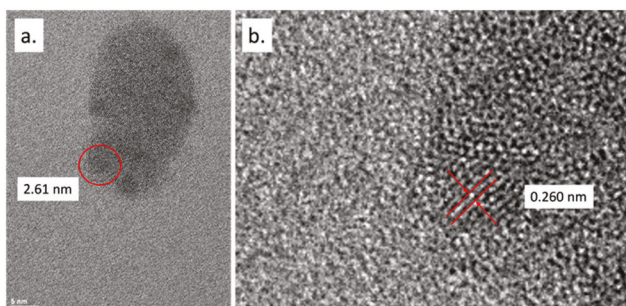


Fig. 1 TEM images of representative BTYA-passivated MHMCs in both an (a) wide view and (b) close view.

the detailed LARP syntheses. Generally, the LARP syntheses follow a standard methodology using *N,N*-dimethylformamide (DMF) and toluene as a solvent and antisolvent, respectively.^{9,10,14} Identical molar amounts of precursor and ligand were used as those listed in the solid syntheses described above.

Fig. 1 shows TEM images of representative MHMCs synthesized in the solid state. Fig. 1a shows that the nanocrystals, measured on average at about 2.1 nm, have size on the same order as the previous study, while Fig. 1b shows a higher resolution image with lattice spacing, measured at 0.260 nm.¹⁵

The consistency in size and lattice spacing when compared with earlier work supports the MHMCs' identification.

Several previous studies of MHMCs show a typical first excitonic absorption band centered around 400 nm, representing a 100 nm blue shift as compared to lead bromide PQDs.^{10,14,15} Thus, UV-Vis and PL data can be reliably used to assess the formation of MHMCs. In Fig. 2a, solid-state MHMC first excitonic absorption and emission features are shown with bands peaking at 404 and 409 nm. To make a direct comparison to the particles produced by the novel synthesis, LARP MHMCs were synthesized. The peak positions of the solid-state MHMCs show excellent agreement with the LARP MHMCs shown in Fig. S1a (ESI[†]) which also have first excitonic absorption and emission at 404 and 409 nm.

To illustrate the spectral differences that occur due to the structural differences between MHMCs and similarly blue-emitting clusters, MAPbBr_3 PMSCs were also synthesized in the solid state. Their first excitonic absorption and emission spectra are shown in Fig. 2b. The first excitonic absorption and emission bands peak at 432 and 445 nm, respectively. While red shifted in relation to the MHMC shown in Fig. 2a, the absorption and emission features are significantly bluer than those of lead bromide PQDs, which typically peak at 500 nm.

The PMSC absorption and PL peak positions are in good agreement with previously described PMSCs synthesized by LARP using OA and OAm for passivation, with a slight difference in peak position attributed to a subtle difference in particle size.⁹ Additionally, the PL band is narrow, with a full width at half maximum (FWHM) of 20 nm. Similarly, the PL peaks of the solid-state and LARP synthesized MHMCs have FWHM measured at 15 and 12 nm, respectively, a feature which is typical of MHMCs due to their narrow size distribution.

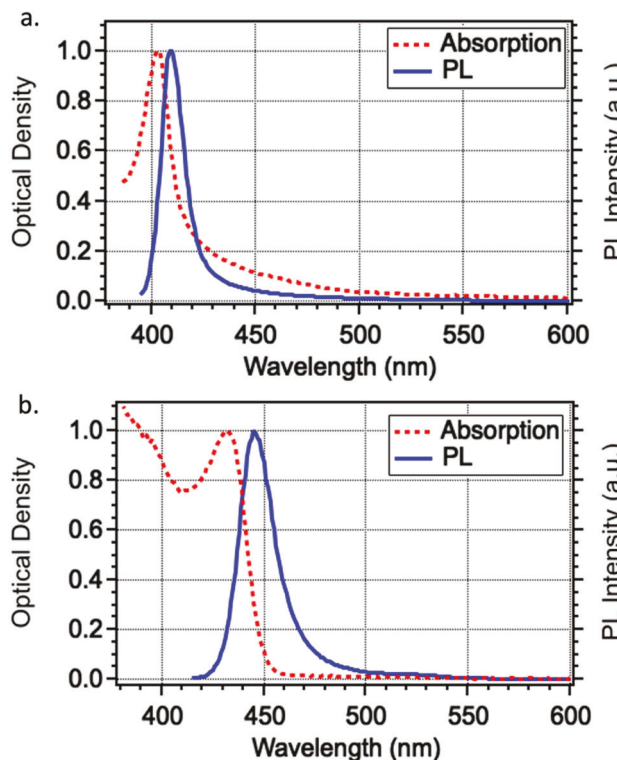


Fig. 2 UV-Vis electronic absorption and PL spectra of (a) solid-state MHMCs with PL excitation at 365 nm, and (b) solid state PMSCs with PL excitation at 400 nm.

Like the PMSCs, agreement in peak position suggests that the MHMCs synthesized by the solid-state method are likely of the same species as the LARP MHMCs, which have been subject to previous optical and structural studies in recent literature.^{10,14,15}

To compare the MHMC crystallinity against previous reports and against the PbBr_2 precursor, X-ray diffraction (XRD) was carried out, as shown in Fig. 3. Here, the MHMCs have been purified by redispersion in toluene with an additional aliquot of BTYA at a rate of 0.6 mg crude product mL^{-1} toluene and diluted at a rate of 20 $\mu\text{L mL}^{-1}$ before drop casting. The XRD shows six product peaks with a regular spacing of about 6.4° , consistent with MHMCs synthesized in past work using LARP.

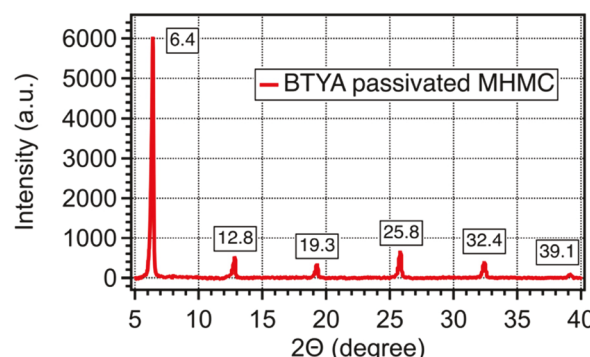


Fig. 3 XRD of BTYA-passivated MHMC powder.

This XRD spectrum was compared to that of the crude MHMC product, as shown in Fig. S3 (ESI†). While purification steps were carried out to determine whether good homogeneity and product purity could be attained, any residual unreacted PbBr_2 is not thought to impact the MHMC spectroscopy. XRD for the PMSCs was carried out similarly to previous work, using paraffin as a stabilizing matrix, shown in Fig. S4 (ESI†). The PMSC XRD peak positions were compared against past work on PMSCs and PQDs and show good agreement. In particular, the peak at 14.9 has been highlighted in earlier work as a key feature. The peak at 21.1, labeled with a spade symbol, is assigned to the paraffin stabilizing matrix as described in earlier work.^{9,19}

In addition to XRD, high-resolution Raman spectroscopy was used to confirm the structural agreement between solid-state and LARP MHMCs. Here, BTYA-passivated MHMCs without an acidic passivating ligand were synthesized in the solid-state grinding method presented above.¹⁵ The Raman spectrum shown in Fig. 4 contains 6 major bands, which are consistent with previously reported BTYA-passivated MHMCs.¹⁵ The peaks at 58, 74, 87, 104, 260, and 322 cm^{-1} are thus assigned to phonon modes summarized in Table S1 (ESI†).

The good agreement in the Raman features between the LARP-synthesized MHMCs and the solid state synthesized MHMCs here is a further indication that these two sets of samples having the same or similar composition and structure. Similarly, the Raman spectrum of the solid state synthesized PMSCs was taken and is shown in Fig. S5 (ESI†). The bands observed in the PMSC Raman spectrum were compared to previous work on PMSCs synthesized by LARP. The strong feature at 220 cm^{-1} is thus attributed to torsional vibration of methylammonium, and the weak feature at 346 cm^{-1} is attributed to a MA-cage mode. The bands observed are consistent with past PMSC work and show a clear difference when compared to the MHMC Raman shown in Fig. 4, which allows for distinction between the two nanoclusters.^{9,15,20}

To gain a better understanding of MHMC behavior in terms of their fluorescence lifetime, TRPL measurements of the MHMCs were taken. The trace, probed at 415 nm, is shown in Fig. 5 in blue and is fit to a two-component exponential decay fit.

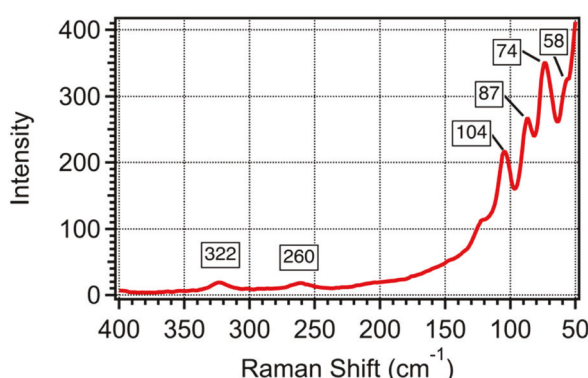


Fig. 4 Raman spectrum of BTYA-passivated MHMCs synthesized in the solid state.

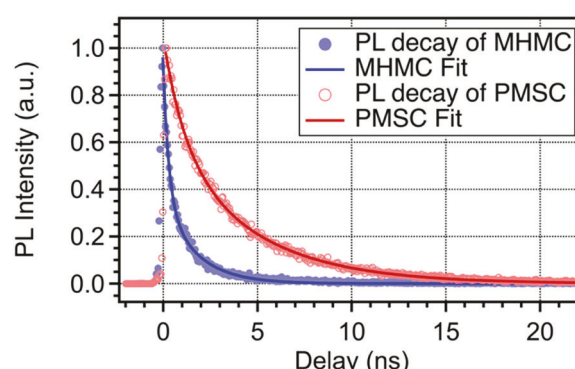


Fig. 5 TRPL trace of BTYA-passivated MHMCs monitored at 415 nm (solid blue), and OA-OAm passivated PMSCs monitored at 445 nm (open red) following excitation at 370 nm.

The MHMCs display a short overall lifetime, where the short and long components are measured at 300 ps and 1.7 ns, respectively. This relatively short overall lifetime indicates a likely defect-rich structure and is expected when considering the low PLQY of 3% and compares well to the fluorescence lifetime of past LARP MHMCs with similarly low PLQY.¹⁶ This is contrasted against the PMSCs, shown in Fig. 5 in red, which have a PLQY of 44%. They show a short component of 1.1 ns and a long component of 4.5 ns, on the same order of magnitude as previously reported PMSCs.²¹

In summary, a novel solid-state synthesis of MHMCs has been demonstrated. Good agreement has been found in the optical absorption and emission features when compared to the more typical LARP synthesis for both PMSCs and MHMCs. Similarly, good agreement was observed in their Raman, XRD, and TRPL spectra. This study demonstrates a simple alternative approach to synthesizing highly confined nanoclusters in a solid state form, which is of interest for many potential applications.

David C. Zeitz: conceptualization, formal analysis, methodology, investigation, validation, and writing – original draft. Kai-Chun Chou: investigation, validation, and writing – review and editing. Jin Z. Zhang: conceptualization, funding acquisition, project administration, supervision, resources, and writing – review and editing.

This work was financially supported by NSF (CHE-2203633). We acknowledge the help of Jeremy Barnett at the UCSC X-ray diffraction facility, Dr Chengyu Song at the National Center for Electron Microscopy, and Mariam Khvichia.

Data availability

The data supporting this article has been included as part of the ESI.†

Conflicts of interest

There are no conflicts to declare.

References

1 J. A. Sichert, Y. Tong, N. Mutz, M. Vollmer, S. Fischer, K. Z. Milowska, R. García Cortadella, B. Nickel, C. Cardenas-Daw, J. K. Stolarczyk, A. S. Urban and J. Feldmann, Quantum Size effect in organometal halide perovskite nanoplatelets, *Nano Lett.*, 2015, 15(10), 6521–6527, DOI: [10.1021/acs.nanolett.5b02985](https://doi.org/10.1021/acs.nanolett.5b02985).

2 Y. Bekenstein, B. A. Koscher, S. W. Eaton, P. Yang and A. P. Alivisatos, Highly Luminescent Colloidal Nanoplates of Perovskite Cesium Lead Halide and Their Oriented Assemblies, *J. Am. Chem. Soc.*, 2015, 137(51), 16008–16011, DOI: [10.1021/jacs.5b11199](https://doi.org/10.1021/jacs.5b11199).

3 Y. Tong, E. Bladt, M. F. Aygüler, A. Manzi, K. Z. Milowska, V. A. Hintermayr, P. Docampo, S. Bals, A. S. Urban, L. Polavarapu and J. Feldmann, Highly Luminescent Cesium Lead Halide Perovskite Nanocrystals with Tunable Composition and Thickness by Ultrasonication, *Angew. Chem., Int. Ed.*, 2016, 55(44), 13887–13892, DOI: [10.1002/anie.201605909](https://doi.org/10.1002/anie.201605909).

4 J. Ghosh, L. P. L. Mawlong, A. J. Pattison, W. Theis, S. Chakraborty and P. K. Giri, Solid-State Synthesis of Stable and Color Tunable Cesium Lead Halide Perovskite Nanocrystals and the Mechanism of High-Performance Photodetection in a Monolayer $\text{MoS}_2/\text{CsPbBr}_3$ Vertical Heterojunction, *J. Mater. Chem. C*, 2020, 8(26), 8917–8934, DOI: [10.1039/DOTC01306D](https://doi.org/10.1039/DOTC01306D).

5 P. Pal, S. Saha, A. Banik, A. Sarkar and K. Biswas, All-Solid-State Mechanochemical Synthesis and Post-Synthetic Transformation of Inorganic Perovskite-Type Halides, *Chem. – Eur. J.*, 2018, 24(8), 1811–1815, DOI: [10.1002/chem.201705682](https://doi.org/10.1002/chem.201705682).

6 K. Tanaka, T. Takahashi, T. Ban, T. Kondo, K. Uchida and N. Miura, Comparative Study on the Excitons in Lead-Halide-Based Perovskite-Type Crystals $\text{CH}_3\text{NH}_3\text{PbBr}_3$ $\text{CH}_3\text{NH}_3\text{PbI}_3$, *Solid State Commun.*, 2003, 127(9), 619–623, DOI: [10.1016/S0038-1098\(03\)00566-0](https://doi.org/10.1016/S0038-1098(03)00566-0).

7 L. Peng, A. Dutta, R. Xie, W. Yang and N. Pradhan, Dot-Wire-Platelet-Cube: Step Growth and Structural Transformations in CsPbBr_3 Perovskite Nanocrystals, *ACS Energy Lett.*, 2018, 3(8), 2014–2020, DOI: [10.1021/acsenergylett.8b01037](https://doi.org/10.1021/acsenergylett.8b01037).

8 T. Udayabhaskararao, M. Kazes, L. Houben, H. Lin and D. Oron, Nucleation, Growth, and Structural Transformations of Perovskite Nanocrystals, *Chem. Mater.*, 2017, 29(3), 1302–1308, DOI: [10.1021/acs.chemmater.6b04841](https://doi.org/10.1021/acs.chemmater.6b04841).

9 M. Guarino-Hotz, J. L. Barnett, K.-C. Chou, A. A. Win, H. Zhang, C. Song, S. R. J. Oliver and J. Z. Zhang, Structural Study of Paraffin-Stabilized Methylammonium Lead Bromide Magic-Sized Clusters, *J. Phys. Chem. C*, 2023, 127(6), 3367–3376, DOI: [10.1021/acs.jpcc.2c08645](https://doi.org/10.1021/acs.jpcc.2c08645).

10 E. T. Vickers, Z. Chen, V. Cherrette, T. Smart, P. Zhang, Y. Ping and J. Z. Zhang, Interplay between Perovskite Magic-Sized Clusters and Amino Lead Halide Molecular Clusters, *Research*, 2021, 2021, 6047971, DOI: [10.3433/2021/6047971](https://doi.org/10.3433/2021/6047971).

11 L. Liu, K. Xu, E. T. Vickers, A. Allen, X. Li, L. Peng and J. Z. Zhang, Varying the Concentration of Organic Acid and Amine Ligands Allows Tuning between Quantum Dots and Magic-Sized Clusters of $\text{CH}_3\text{NH}_3\text{PbBr}_3$ Perovskite: Implications for Photonics and Energy Conversion, *ACS Appl. Nano Mater.*, 2020, 3(12), 12379–12387, DOI: [10.1021/acsanm.0c02894](https://doi.org/10.1021/acsanm.0c02894).

12 K. Xu, A. C. Allen, B. Luo, E. T. Vickers, Q. Wang, W. R. Hollingsworth, A. L. Ayzner, X. Li and J. Z. Zhang, Tuning from Quantum Dots to Magic Sized Clusters of CsPbBr_3 Using Novel Planar Ligands Based on the Trivalent Nitrate Coordination Complex, *J. Phys. Chem. Lett.*, 2019, 10(15), 4409–4416, DOI: [10.1021/acs.jpclett.9b01738](https://doi.org/10.1021/acs.jpclett.9b01738).

13 L. Protesescu, S. Yakunin, M. I. Bodnarchuk, F. Krieg, R. Caputo, C. H. Hendon, R. X. Yang, A. Walsh and M. V. Kovalenko, Nanocrystals of Cesium Lead Halide Perovskites (CsPbX_3 , X = Cl, Br, and I): Novel Optoelectronic Materials Showing Bright Emission with Wide Color Gamut, *Nano Lett.*, 2015, 15(6), 3692–3696, DOI: [10.1021/nl5048779](https://doi.org/10.1021/nl5048779).

14 A. A. Win, K.-C. Chou, D. C. Zeitz, C. Todd and J. Z. Zhang, Origin of the near 400 nm Absorption and Emission Band in the Synthesis of Cesium Lead Bromide Nanostructures: Metal Halide Molecular Clusters Rather Than Perovskite Magic-Sized Clusters, *J. Phys. Chem. Lett.*, 2023, 14(1), 116–121, DOI: [10.1021/acs.jpclett.2c03734](https://doi.org/10.1021/acs.jpclett.2c03734).

15 H. Zhang, E. T. Vickers, S. Erickson, M. Guarino-Hotz, J. L. Barnett, S. Ghosh and J. Z. Zhang, Synthesis and Properties of Stable Amino Metal Halide Molecular Clusters in the Solid State, *J. Phys. Chem. Lett.*, 2022, 13(45), 10543–10549, DOI: [10.1021/acs.jpclett.2c02977](https://doi.org/10.1021/acs.jpclett.2c02977).

16 H. Zhang, D. C. Zeitz and J. Z. Zhang, Ultrafast Study of Excited State Dynamics of Amino Metal Halide Molecular Clusters, *J. Phys. Chem. Lett.*, 2023, 14(36), 8095–8099, DOI: [10.1021/acs.jpclett.3c01952](https://doi.org/10.1021/acs.jpclett.3c01952).

17 C. F. Todd and J. Z. Zhang, Novel Chiral CsPbBr_3 Metal Halide Perovskite Magic-Sized Clusters and Metal Halide Molecular Clusters with Achiral Ligands, *J. Phys. Chem. Lett.*, 2023, 10630–10633, DOI: [10.1021/acs.jpclett.3c02581](https://doi.org/10.1021/acs.jpclett.3c02581).

18 P. Liu, W. Chen, Y. Okazaki, Y. Battie, L. Brocard, M. Decossas, E. Pouget, P. Müller-Buschbaum, B. Kauffmann, S. Pathan, T. Sagawa and R. Oda, Optically Active Perovskite CsPbBr_3 Nanocrystals Helically Arranged on Inorganic Silica Nanohelices, *Nano Lett.*, 2020, 20(12), 8453–8460, DOI: [10.1021/acs.nanolett.0c02013](https://doi.org/10.1021/acs.nanolett.0c02013).

19 K.-H. Wang, L.-C. Li, M. Shellaiah and K. Wen Sun, Structural and Photophysical Properties of Methylammonium Lead Tribromide (MAPbBr_3) Single Crystals, *Sci. Rep.*, 2017, 7(1), 13643, DOI: [10.1038/s41598-017-13571-1](https://doi.org/10.1038/s41598-017-13571-1).

20 M. Mączka and M. Ptak, Temperature-Dependent Raman Studies of FAPbBr_3 and MAPbBr_3 Perovskites: Effect of Phase Transitions on Molecular Dynamics and Lattice Distortion, *Solids*, 2022, 3(1), 111–121, DOI: [10.3390/solids3010008](https://doi.org/10.3390/solids3010008).

21 D. C. Zeitz, V. L. Cherrette, S. A. Creech, Y. Li, Y. Ping and J. Z. Zhang, Ultrafast Spin Relaxation of Charge Carriers in Strongly Quantum Confined Methylammonium Lead Bromide Perovskite Magic-Sized Clusters, *ACS Phys. Chem. Au*, 2024, DOI: [10.1021/acsphyschemau.4c00051](https://doi.org/10.1021/acsphyschemau.4c00051).